IMAGE ENHANCEMENT VIA EXTRAPOLATION TECHNIQUES: A TWO DIMENSIONAL ITERATIVE SCHEME A DIRECT MATRIX INVERSION SCHEME

L. David Sabbagh, Harold A. Sabbagh and James S. Klopfenstein

Sabbagh Associates, Inc.
2634 Round Hill Lane
Bloomington, IN 47401

INTRODUCTION

In [1] and [2], we have developed a model and three dimensional inversion algorithm for detecting flaw in structures. The model, based on rigorous electromagnetic theory, and the algorithm have as their main objective the high resolution imaging of the flaw. The algorithm is computationally intensive and, like other inversion techniques, involves the solution of some ill conditioned problems.

The major computations for our implementation of the algorithm are done in the two dimensional frequency domain. In order to take an inverse Fourier transform, we must solve a system of equations for each spatial frequency pair (k_x, k_y). For large values of (k_x, k_y), the system matrix becomes highly ill conditioned; hence solving the system for these values of (k_x, k_y) becomes impractical.

While the system is ill conditioned at all frequencies, the inevitable filtering of the high frequency spectral components in the system matrix causes particular problems. For small values of (k_x, k_y), the solution of our system gives good information in the Fourier domain. However, in order to achieve high resolution reconstructions, these missing high frequency components, which may be present in the in the solution, are needed. Thus we need a method that will allow us to get this information.

To get this missing high frequency information, we use a powerful mathematical tool called analytic continuation. This paper discusses two approaches to analytic continuation, the first utilizing a two dimensional iterative scheme based on the technique of projection onto convex sets, [3]-[7], and the second utilizing a direct matrix inversion technique, [8]-[10]. An important feature of the first method is that *a priori* knowledge about the unknown can be incorporated into the reconstruction technique in a natural way. Such information includes the finite support and/or constraints. We also give results of simulated flaws.

MATHEMATICAL BACKGROUND

Our Analytic continuation method is based on the following two theorems that are well known in complex and Fourier analysis.

Theorem 1. *The two-dimensional Fourier transform of a spatially bounded function is an analytic function in the* (k_x, k_y)*-plane.*

Theorem 2. *If any analytic function in the* (k_x, k_y)*-plane is known exactly in an arbitrarily small (nonzero) region of that plane, then the entire function can be found (uniquely) by means of analytic continuation.*

In order to use these theorems, we recall that a flaw can be thought of as a space-limited function $g(x,y)$ (or a function with compact support). Thus, by Theorem 1, its Fourier transform, $G(k_x, k_y)$, is analytic in the (k_x, k_y)-plane. If we have only limited information about G, say, only its values at low spatial-frequencies, Theorem 2 tells us that we can uniquely extend G to the whole (k_x, k_y)-plane. Once we have continued G to the (k_x, k_y)-plane, we can take an inverse Fourier transform to recover g.

AN ITERATIVE SCHEME FOR ANALYTIC CONTINUATION

The mathematical setting for the algorithm is projections onto closed linear manifolds (CLM) in a Hilbert space. Important features of the method include:

1. *a priori* knowledge about g can be incorporated into the reconstruction technique in a natural way.
2. Such information includes the finite support and/or any constraints.
3. In our application we know that the conductivity within the anomalous region is bounded, which in our model implies that $-1 \leq g(x,y) \leq 0$, and we also have an estimate of the support of g.

The algorithm that we used is listed here:

ALGORITHM

Let the function $G(k_x, k_y)$ be given over a prescribed region $\mathcal{L}$, and let $\mathcal{F}$ be the Fourier transform. Then starting with:

$$f_0(x,y) = \mathcal{F}^{-1}[G(k_x, k_y)];$$
$$r = 0;$$

REPEAT

$$f_r^{(1)} = P_1 f_r;$$
$$f_r^{(2)} = P_3 f_r^{(1)};$$
$$F_{r+1}^{(1)} = \mathcal{F}[f_r^{(2)}];$$
$$F_{r+1} = P_2 F_{r+1}^{(1)};$$
$$f_{r+1} = \mathcal{F}^{-1}[F_{r+1}];$$
$$r = r + 1;$$

UNTIL CONVERGENCE OCCURS.

The important operations in the Algorithm are the Fourier and inverse Fourier transforms and the various projection operators P_i, which we now define:

$$P_1 f = \begin{cases} f, & (x,y) \in S, \quad S = \text{support of } f, \\ 0, & \text{otherwise.} \end{cases}$$

$$P_2 F = \begin{cases} G(k_x,k_y), & (k_x,k_y) \in \mathcal{L}, \\ F(k_x,k_y), & (k_x,k_y) \notin \mathcal{L}, \text{ where } F(k_x,k_y) = \mathcal{F}[f(x,y)] \end{cases}$$

$$P_3 f = \begin{cases} -1, & \text{if } f(x,y) < -1 \\ f(x,y), & \text{if } -1 \le f(x,y) \le 0 \\ 0, & \text{if } f(x,y) > 0 \end{cases}$$

Hence, the algorithm successively applies the known properties of the sought-for solution to the initial given data. Numerical experiments suggest various methods for speeding the convergence.

A DIRECT MATRIX INVERSION SCHEME FOR ANALYTIC CONTINUATION

The basis for this technique is the Whittaker-Shannon Sampling Theorem which we briefly discuss. Let $g(x,y)$ have spectrum $G(k_x,k_y)$, and let G be sampled in Fourier space with periods δF_x, δF_y in the k_x and k_y directions, respectively. Then

$$G(k_x,k_y) = \begin{aligned} &4L_xL_y\delta F_x\delta F_y \textstyle\sum_{n=-\infty}^{\infty}\sum_{m=-\infty}^{\infty} G(n\delta F_x, m\delta F_y)\times \\ &\operatorname{sinc}[2L_x(k_x - n\delta F_x)]\operatorname{sinc}[2L_y(k_y - m\delta F_y)] \end{aligned}$$

where $\operatorname{sinc}(x) = \sin(\pi x)/\pi x$ is the Fourier transform of the rect function, which is unity when its argument lies within -1/2 to +1/2. Note that, if $g_s(x,y)$ is the sampled version of $g(x,y)$, whose support is $2L_x \times 2L_y$, then

$$g(x,y) = \operatorname{rect}[\frac{x}{2L_x}]\operatorname{rect}[\frac{y}{2L_y}]g_s(x,y).$$

Using the Whittaker-Shannon theorem, we derive the matrix equations needed for extrapolation. Letting $f_x = k\delta F_x$ and $f_y = l\delta F_y$, we have

$$G(k\delta F_x, l\delta F_y) = \begin{aligned} &4L_xL_y\delta F_x\delta F_y \textstyle\sum_{n=-\infty}^{\infty}\sum_{m=-\infty}^{\infty} G(n\delta F_x, m\delta F_y)\times \\ &\operatorname{sinc}[2L_x\delta F_x(k-n)]\operatorname{sinc}[2L_y\delta F_y(l-m)]. \end{aligned}$$

Note that this is the direct product of an (infinite) x-matrix and an (infinite) y-matrix.

Now consider truncated one-dimensional matrix equation

$$G_m = \sum_{n=-N}^{N} G_n \frac{\sin[2\pi S_x(m-n)]}{\pi(m-n)}, \qquad m = -M, \ldots, M$$

where S_x is the support in the x-direction and $M \ll N$; hence, the system is strongly underdetermined. Since the system is nonsquare, the solution is not unique. Thus we seek the (unique) minimum norm least squares solution.

The minimum norm solution of the least-squares problem

$$\overline{\overline{B}}\bar{x} \cong \bar{b}$$

is given by the singular value expansion

$$\bar{x} = \overline{\overline{V}}\bar{p}$$

where $\overline{\overline{V}}$ is the matrix of right singular vectors of $\overline{\overline{B}}$;

$$p_i = (\overline{\overline{U}}^T \bar{b})_i / s_i$$

where $\overline{\overline{U}}$ is the matrix of left singular vectors of $\overline{\overline{B}}$;

$\{s_i\}$ are the singular values of $\overline{\overline{B}}$.

Since the high order singular values are small, this problem is highly ill-conditioned. Thus we must not use these high order singular values which means that we do a truncated singular value expansion.

The extension to two dimensional problems is straight forward when it is recognized that all two dimensional singular vectors are direct products of one dimensional singular vectors and the two dimensional singular values are products of one dimensional singular values.

In some situations, the condition of the problem can be improved by 'preconditioning' the system matrix. We used a method of 'derivative smoothing' which we present below.

Consider the one dimensional problem:

$$\min_x \|Ax - b\|^2 + \lambda^2 \|Dx\|^2$$

where D is a discrete derivative operator. If we let $y = Dx$, we get

$$\min_y \|AD^{-1}y - b\|^2 + \lambda^2 \|y\|^2.$$

To solve this, we use the Singular Value Decomposition of the matrix AD^{-1} and then proceed as before. λ is a Levenberg-Marquardt parameter.

We considered two cases. In case one, D is a discrete first derivative operator

$$D = \begin{pmatrix} 1 & 0 & \dots & 0 & 0 \\ -1 & 1 & \dots & 0 & 0 \\ \vdots & \vdots & \ddots & \vdots & \vdots \\ 0 & 0 & \dots & 1 & 0 \\ 0 & 0 & \dots & -1 & 1 \end{pmatrix}$$

and

$$D^{-1} = \begin{pmatrix} 1 & \dots & 0 \\ \vdots & \ddots & \vdots \\ 1 & \dots & 1 \end{pmatrix}$$

In case two, D is a symmetric discrete second derivative operator

$$D = \frac{1}{h^2} \begin{pmatrix} -2 & 1 & 0 & \dots & 0 & 0 \\ 1 & -2 & 1 & \ddots & 0 & 0 \\ 0 & 1 & -2 & \ddots & 0 & 0 \\ \vdots & \ddots & \ddots & \ddots & \ddots & \vdots \\ 0 & 0 & 0 & \ddots & -2 & 1 \\ 0 & 0 & 0 & \dots & 1 & -2 \end{pmatrix}$$

RESULTS

We performed numerical experiments on three flaws:

- Flaw 1 was an impulse,
- Flaw 2 was a pulse, and
- Flaw 3 was a structured flaw.

Figures 1, 2 and 3 show these flaws both as three dimensional and gray scale pictures.

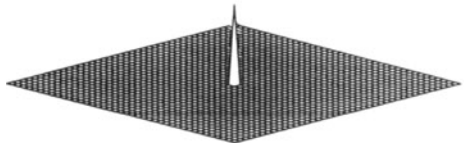

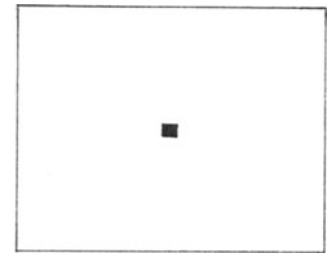

Fig. 1. Three dimensional and gray scale representation of Flaw 1.

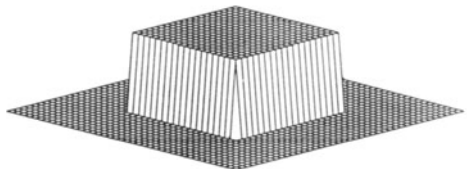

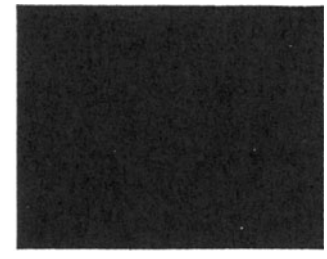

Fig. 2. Three dimensional and gray scale representation of Flaw 2.

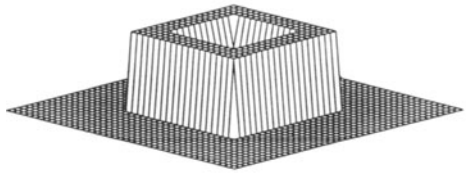

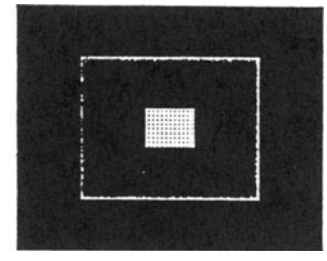

Fig. 3. Three dimensional and gray scale representation of Flaw 3.

Before describing the results, let us give names to the reconstruction methods:

- Method 1 was using the inverse Fourier transform directly,
- Method 2 was the iterative extrapolation technique, called LENTUY,
- Method 3 was the matrix inverse technique with no smoothing, called SVA2DO, and
- Method 4 was the matrix inverse technique with symmetric second derivative smoothing, called SVA2DSY.

Figure 4 shows the reconstruction of Flaw 1 using Method 1 on the lowest 61 out of 256 frequencies in both the k_x and k_y directions. In this case, no extrapolation of data was used. Figure 5 shows the reconstruction of Flaw 1 using Method 2 on the lowest 61 frequencies and 10 iterations. Figure 6 shows the reconstruction of Flaw 1 using Method 3 with $M = 10$ and using the first 7 singular values. Figure 7 shows the reconstruction of Flaw 1 using Method 4 with $M = 10$ and using the first 6 singular values.

[Note: Some gray scale representations of these flaws have been omitted in these figures since they are too small for reproduction. The Editors]

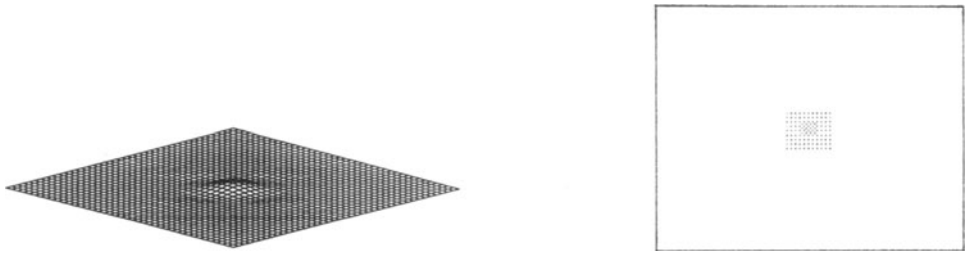

Fig. 4. Three dimensional representation of Flaw 1 using Method 1.

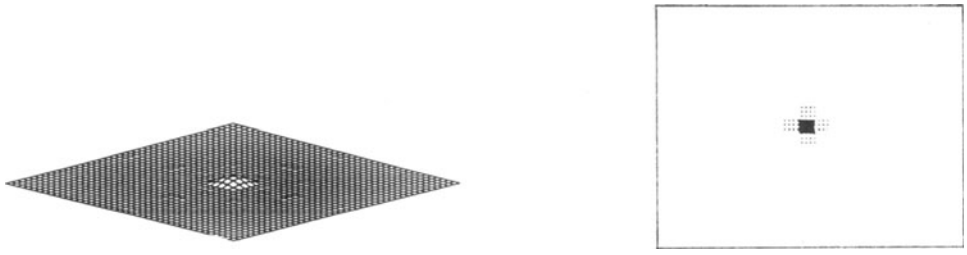

Fig. 5. Three dimensional

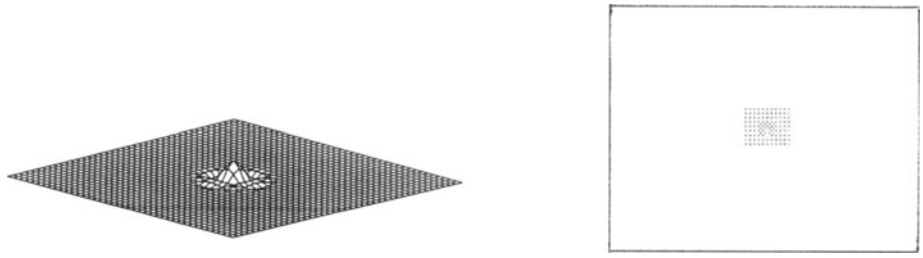

Fig. 6. Three dimensional and gray scale representation of Flaw 1 using Method 3.

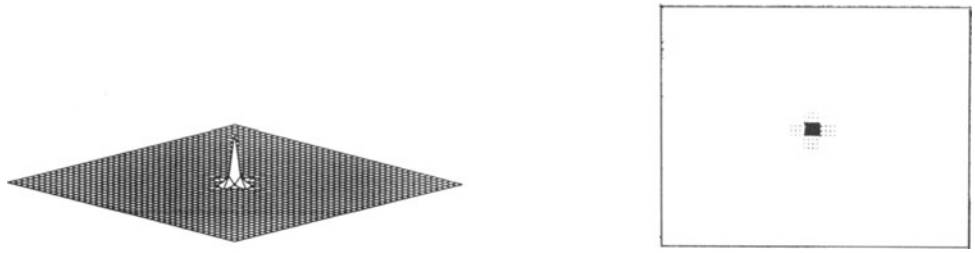

Fig. 7. Three dimensional and gray scale representation of Flaw 1 using Method 4.

Figures 8, 9 and 10 show the reconstructions of Flaw 2 using Methods 1, 2 and 3, respectively. Methods 1 and 2 both use the lowest 61 frequencies and Method 2 goes through 10 iterations, while Method 3 has $M = 10$ and uses the first 14 singular values.

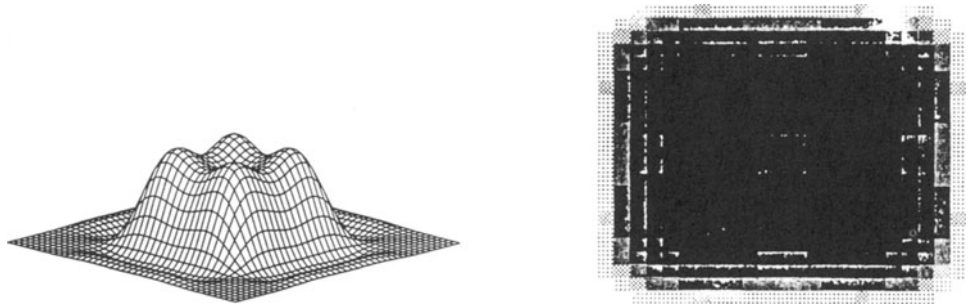

Fig. 8. Three dimensional and gray scale representation of Flaw 2 using Method 1.

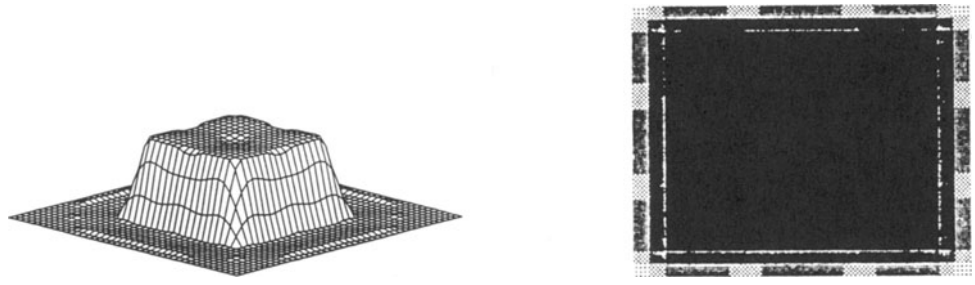

Fig. 9. Three dimensional and gray scale representation of Flaw 2 using Method 2.

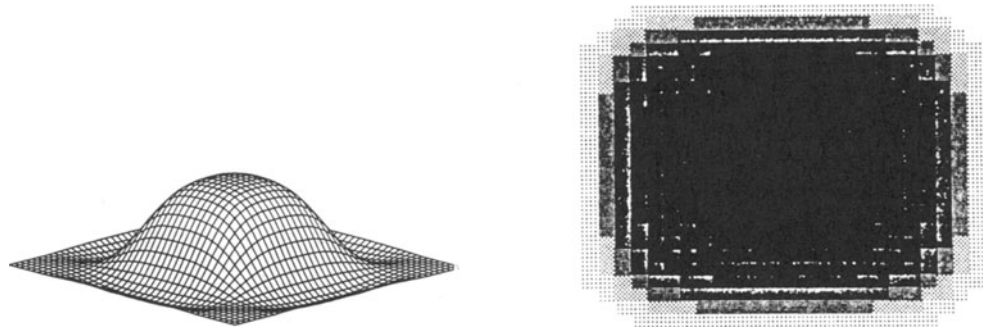

Fig. 10. Three dimensional and gray scale representation of Flaw 2 using Method 3.

Figures 11, 12 and 13 show the reconstructions of Flaw 3 again using Methods 1, 2 and 3, respectively. Methods 1 and 2 again use the lowest 61 frequencies and Method 2 again uses 10 iterations, while Method 3 again has $M = 10$ and uses the first 14 singular values.

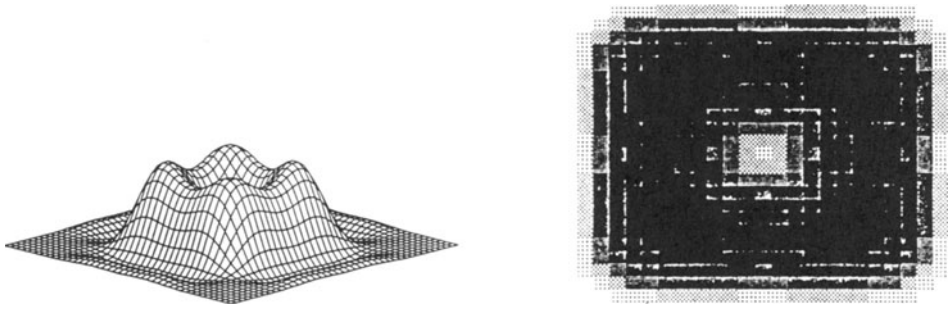

Fig. 11. Three dimensional and gray scale representation of Flaw 3 using Method 1.

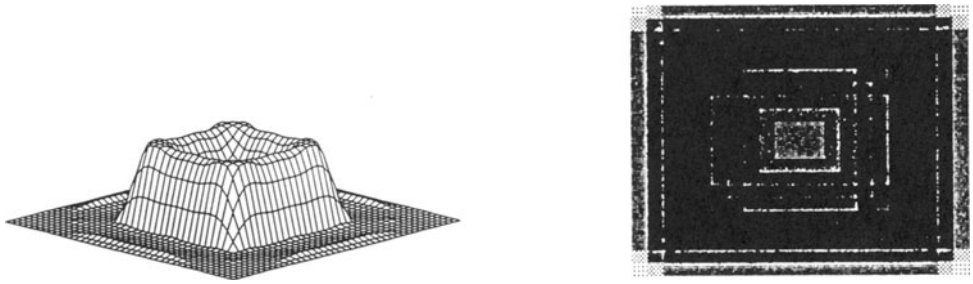

Fig. 12. Three dimensional and gray scale representation of Flaw 3 using Method 2.

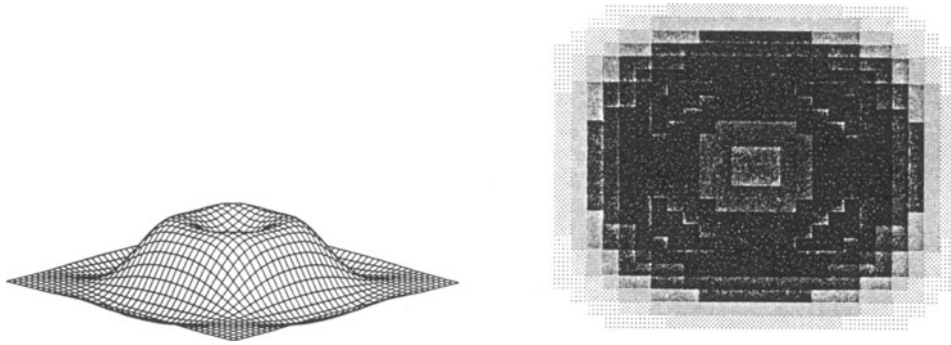

Fig. 13. Three dimensional and gray scale representation of Flaw 3 using Method 3.

As we can see from these results, the extrapolation techniques enhance the reconstructions of these flaws. The matrix method may be better for the impulsive flaw, but the iterative method is better for the other flaws. In addition, in the iterative method, it is easier to include *a priori* data.

ACKNOWLEDGEMENT

This work was supported by the Department of Energy under Contract No. DE-AC02-83-ER80096 with Sabbagh Associates, Inc.

REFERENCES

1. H. A. Sabbagh and L. D. Sabbagh, ''Development of an Eddy-Current Sensor and Algorithm for Three-Dimensional Quantitative Non-Destructive Evaluation,'' Final Report Contract No. DE-AC02-83ER80096 with U.S. Department of Energy.

2. L. D. Sabbagh and H. A. Sabbagh, *Review of Progress in Quantitative Nondestructive Evaluation* 4A, D. O. Thompson and D. E. Chimenti, Eds., (Plenum Press, New York, 1984), pp. 635-642.

3. A. Papoulis, ''A New Algorithm in Spectral Analysis and Band-Limited Extrapolation,'' IEEE Trans. Circuit Syst., vol CAS-22, pp. 735-742, 1975.

4. Dante C. Youla, ''Generalized Image Restoration by the Method of Alternating Orthognal Projections,'' IEEE Trans. Circuits Syst., vol CAS-25, pp. 694-702, 1978.

5. D. C. Youla and H. Webb, ''Image Restoration by the Method of Convex Projections: Part 1--Theory,'' IEEE Transactions on Medical Imaging, vol MI-1, pp. 81-94, October 1982.

6. M. I. Sezan and H. Stark, ''Image Restoration by the Method of Convex Projections: Part 2--Applications and Numerical Results,'' IEEE Transactions on Medical Imaging, vol MI-1, pp. 95-101, October 1982.

7. A. Lent and H. Tuy, ''An Iterative Method for the Extrapolation of Band Limited Functions,'' J. Math. Anal. Appl., vol 83, pp. 554-565, 1981.

8. B. J. Sullivan and B. Liu, ''On the Use of Singular Value Decomposition and Decimation in Discrete-Time Band-Limited Signal Extrapolation,'' IEEE Trans. on Acoustics, Speech, and Signal Processing, vol ASSP-32, No. 6, December 1984.

9. A. K. Jain and S. Ranganath, ''Extrapolation Algorithms For Discrete Signals with Application in Spectral Estimation,'' IEEE Trans. Acoustics, Speech, and Signal Processing, vol ASSP-29, No. 4, August 1981, pp. 830-845.

10. Y. S. Shim and Z. H. Cho, ''SVD Pseudoinversion Image Reconstruction,'' IEEE Trans. Acoustics, Speech, and Signal Processing, vol ASSP-29, No. 4, August 1981, pp. 904-909.